Liquid-Liquid Transition in a Bose Fluid near Collapse

Saverio Moroni,[1,*] Fabio Cinti,[2,3,4,†] Massimo Boninsegni,[5,‡] Giuseppe Pellicane,[6,7,8,§] and Santi Prestipino[9,‖]
[1]CNR-IOM DEMOCRITOS, Istituto Officina dei Materiali and SISSA Scuola Internazionale Superiore di Studi Avanzati, Via Bonomea 265, I-34136 Trieste, Italy
[2]Dipartimento di Fisica e Astronomia, Università di Firenze, I-50019 Sesto Fiorentino (FI), Italy
[3]INFN, Sezione di Firenze, I-50019 Sesto Fiorentino (FI), Italy
[4]Department of Physics, University of Johannesburg, P.O. Box 524, Auckland Park 2006, South Africa
[5]Department of Physics, University of Alberta, Edmonton, Alberta T6G 2H5, Canada
[6]Dipartimento di Scienze Biomediche, Odontoiatriche e delle Immagini Morfologiche e Funzionali, Università degli Studi di Messina, I-98125 Messina, Italy
[7]National Institute of Theoretical and Computational Sciences (NIThECS), 3209 Pietermaritzburg, South Africa
[8]School of Chemistry and Physics, University of Kwazulu-Natal, 3209 Pietermaritzburg, South Africa
[9]Dipartimento di Scienze Matematiche e Informatiche, Scienze Fisiche e Scienze della Terra, Università degli Studi di Messina, viale F. Stagno d'Alcontres 31, I-98166 Messina, Italy

(Received 29 February 2024; accepted 18 July 2024; published 26 August 2024)

Discovering novel emergent behavior in quantum many-body systems is a main objective of contemporary research. In this Letter, we explore the effects on phases and phase transitions of the proximity to a Ruelle-Fisher instability, marking the transition to a collapsed state. To accomplish this, we study by quantum Monte Carlo simulations a two-dimensional system of soft-core bosons interacting through an isotropic finite-ranged attraction, with a parameter η describing its strength. If η exceeds a characteristic value η_c, the thermodynamic limit is lost, as the system becomes unstable against collapse. We investigate the phase diagram of the model for $\eta \lesssim \eta_c$, finding—in addition to a liquid-vapor transition—a first-order transition between two liquid phases. Upon cooling, the high-density liquid turns superfluid, possibly above the vapor-liquid-liquid triple temperature. As η approaches η_c, the stability region of the high-density liquid is shifted to increasingly higher densities, a behavior at variance with distinguishable quantum or classical particles. Finally, for η larger than η_c our simulations yield evidence of collapse of the low-temperature fluid for any density; the collapsed system forms a circular cluster whose radius is insensitive to the number of particles.

DOI: 10.1103/PhysRevLett.133.096001

A first-order transition between two liquid phases is an uncommon, still elusive phenomenon that challenges our understanding of the fluid state of matter [1]. In pure systems, a liquid-liquid phase transition (LLPT) is found in tetrahedral liquids [2,3], where, however, it falls in the supercooled region. A LLPT may occur in parallel with a change in the chemical nature of the constituent particles, like in hydrogen [4], where a molecular liquid is transformed under pressure into an atomic liquid. In equilibrium, a LLPT has been observed in phosphorus [5,6] and in sulfur [7], between liquids characterized by a different degree of polymerization. There also exist (controversial) examples of LLPT in complex molecular fluids (e.g., in triphenyl phosphite [8]). The situation is clearer in models, where a genuine LLPT occurs in classical particles interacting through isotropic core-softened potentials [9–11] or anisotropic potentials [12–14]. The mechanism commonly invoked for the onset of a LLPT is the existence of two distinct repulsive length scales in the effective interparticle potential.

We here introduce a new paradigm of LLPT with no classical counterpart—that is, a structural transition not involving a change in the elementary constituents and/or interactions. To this aim, we push our system (a bosonic fluid) close to its stability threshold, such as existing for particles that interact via a finite repulsion augmented with a strong enough attraction. We will highlight the nontrivial role of quantum indistinguishability, without which the LLPT simply vanishes. In the same system, we also document a first-order transition from liquid to superfluid, a possibility which has remained unexplored so far.

While bare interatomic forces are strongly repulsive at short distances, an effective steplike repulsion can be induced at larger separations, in the nanometer to micrometer range. This is achieved, for instance, in ultracold

*Contact author: moroni@democritos.it
†Contact author: fabio.cinti@unifi.it
‡Contact author: m.boninsegni@ualberta.ca
§Contact author: giuseppe.pellicane@unime.it
‖Contact author: sprestipino@unime.it

bosonic gases, by means of a weak laser coupling of the atomic ground state to a highly excited Rydberg state [15,16]. Such "soft-core" bosons are an ideal playground for the study of supersolidity [17–19], which in this kind of systems is promoted by cluster-crystal ordering of particles at high density [20–23].

We consider the scenario (which could become feasible in future experimental protocols) in which a finite-range attraction of tunable strength is added to a soft-core repulsion. As the strength of attraction grows a Bose fluid eventually undergoes the collapsing transition predicted a long time ago by Ruelle and Fisher [24,25] and observed in classical fluids [26–29].

For a stable interaction (see p. 33 of Ref. [25]), the grand-canonical partition function cannot grow faster than $\exp(cV)$ as a function of the system volume V, where c depends on the temperature and the chemical potential. When stability is violated, the grand partition function is instead divergent, even for finite V, while a system with a fixed number N of particles collapses to a compact cluster or blob with a potential energy proportional to N^2. Ruelle and Fisher derived analytic criteria [24,25] to ascertain whether a bounded potential with an attractive component leads to collapse in a classical system. For a large class of regular potentials, they also proved [24] that classical instability and quantum instability are reciprocally implied in the case of bosons. However, the behavior of a quantum fluid near and beyond the stability threshold is largely unexplored, and can certainly be elucidated by numerical simulation. From the experimental standpoint, the physics of a quantum system near collapse is relevant, for example, to cold dipolar assemblies [30,31].

In this Letter, we present the results of a numerical investigation of a two-dimensional (2D) system of identical particles of spin zero, hence obeying Bose statistics, interacting via a double-Gaussian (DG) potential [28]:

$$u(r) = \epsilon\left[e^{-(r/\sigma)^2} - \eta e^{-(r/\sigma-3)^2}\right], \tag{1}$$

with $\eta > 0$ [we also set a cutoff distance $r_c = 6\sigma$, beyond which $u = 0$ in Eq. (1)]. This potential is known to characterize a fluid near collapse; it has the advantage that the collapsing threshold can be exactly determined (see below). Henceforth, we take ϵ and σ as units of energy and length, respectively. Moreover, the temperature T is expressed in units of ϵ (we set Boltzmann's constant $k_B = 1$).

For an isotropic potential $u(r)$ of finite strength, a sufficient condition for thermodynamic instability is $\tilde{u}(0) < 0$ [25], where $\tilde{u}(k)$ is the Fourier transform of $u(r)$; on the other hand, if $\tilde{u}(k) \geq 0$ for all k, then the system is stable [24]. This implies that, with the DG potential [Eq. (1)], a system is thermodynamically stable for $\eta \leq \eta_c = 0.094\,031\ldots$, unstable for $\eta > \eta_c$.

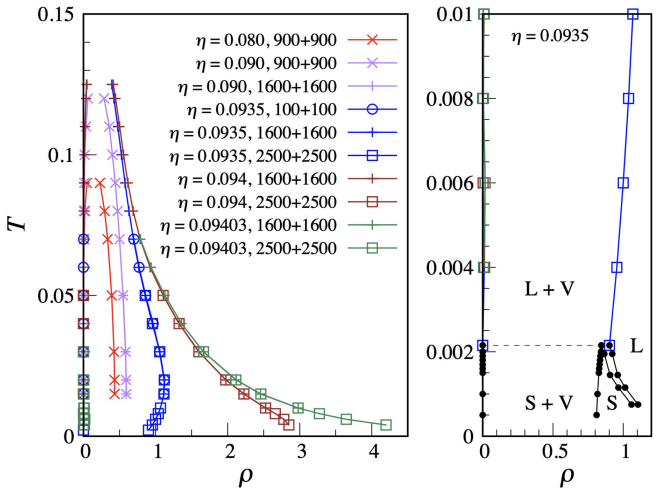

FIG. 1. Phase diagram of the two-dimensional classical DG model on the ρ-T plane. Left: liquid-vapor coexistence data for a few values of $\eta < \eta_c$ and various choices of the initial numbers of particles in the two simulation boxes (in the legend). Right: magnification of the low-temperature region for $\eta = 0.0935$. The triangular solid (S) is stable in a small density window, bounded to the left by the vapor (V) and to the right by the liquid (L). The dashed line marks the triple temperature.

We carried out Monte Carlo simulations of the DG fluid with the aim of exploring—well beyond the usual dilute limit—the route toward Ruelle-Fisher instability in a quantum system, contrasting the system behavior with that of its classical counterpart. By simulating the system beyond the collapse threshold, we also searched for indications of subextensive scaling of the emerging cluster. Our study is completed by an analysis of the structure and superfluidity of the collapsed system, also in comparison with a liquid droplet in equilibrium with vapor.

To set the stage for subsequent analysis, it is useful to investigate first the classical DG fluid as a function of η. We employ Gibbs-ensemble Monte Carlo (GEMC) simulations [32,33] to determine liquid-vapor coexistence and isothermal-isobaric MC simulations to locate the stability region of the triangular crystal. To this purpose, a large-size crystal is heated isobarically until a jump is observed in the values of the number density (ρ) and energy (E).

Liquid-vapor coexistence points for a number of η values close below η_c are plotted in Fig. 1 left. Up to $\eta \approx 0.09$ the shape of the binodal line is usual. As η approaches η_c, however, the coexistence region becomes wider and wider near zero temperature, thus progressively eroding the solid region (whose boundaries are less sensitive to η [34,35]). In particular, notice the substantial increase in width of the two-phase region on going from $\eta = 0.094$ to $\eta = 0.094\,03$ (a value only 3×10^{-5} higher), suggesting that the liquid density diverges as $\eta \to \eta_c$ and $T \to 0$ simultaneously. For $\eta = 0.0935$, where the density of the saturated liquid is around 1, the solid is confined to a tiny region close to $T = 0$ (Fig. 1 right), which would shrink even further for

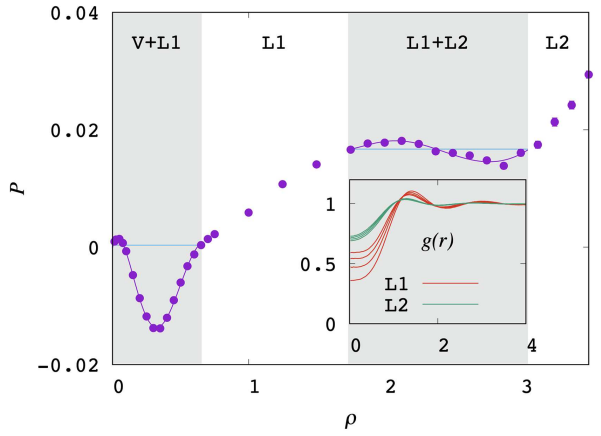

FIG. 2. Pressure versus density for the quantum DG model with $\eta = 0.0935$ at $T = 0.08$. The gray bands are phase-coexistence regions, located by applying the equal-area rule to the P vs $1/\rho$ curve. Inset: PCF of $L1$ and $L2$ at a few densities (between 1 and 1.75 for $L1$; between 3 and 3.75 for $L2$).

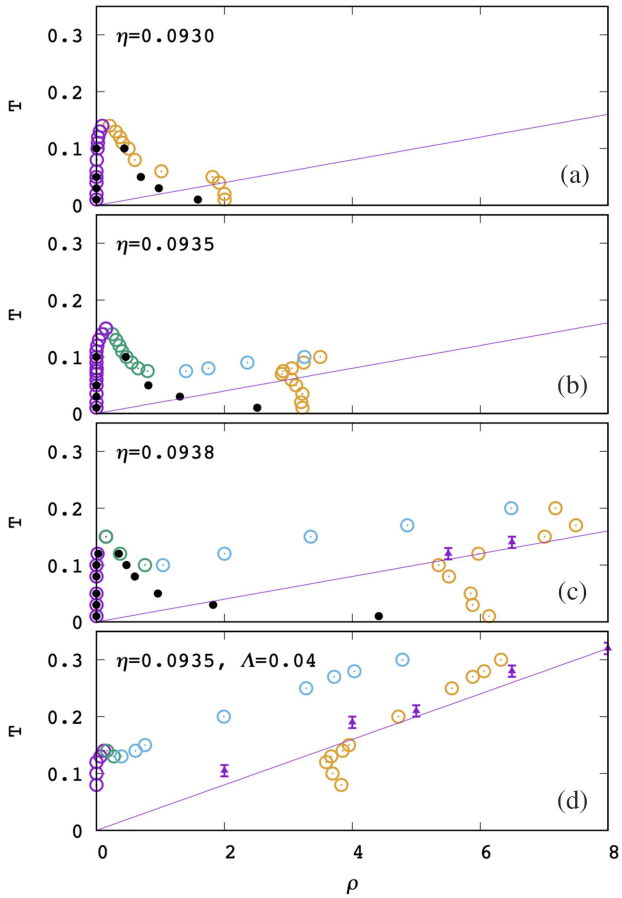

FIG. 3. Phase diagram of the two-dimensional quantum DG model for $\Lambda = 0.02$ and three values of η: 0.093 (a), 0.0935 (b), and 0.0938 (c). In panel (d), $\Lambda = 0.04$ and $\eta = 0.0935$. The circles are coexistence points which are colored differently depending on the phase and the transition involved (see text). Black dots refer to distinguishable particles. Also shown are the straight lines $T = \Lambda\rho$ (see text). A few points on the BKT line are plotted as triangles. The solid phase, if it exists at all, would only be stable at temperatures lower than 0.01.

larger η. We did not observe a hexatic phase, whose existence is possible in an extremely narrow temperature range (no more than 10^{-4} wide) above the solid phase [36], and thus tentatively assume a first-order melting transition. We found no evidence of cluster solids, consistently with the predictions of Ref. [37]. More results for the classical DG fluid, including a survey of the structure of two-phase coexistence at low temperature, are presented in Supplemental Material [38] (see also Refs. [39–41] therein).

For the simulations of the quantum system, we used the continuous-space worm algorithm [42,43]. If periodic boundary conditions are adopted, we compute the superfluid fraction f_s using the winding-number estimator [44]; otherwise, in a droplet regime, we employ the area estimator [45,46]. The relative importance of quantum effects is embodied [47,48] in the parameter $\Lambda = \hbar^2/(m\epsilon\sigma^2)$, m being the particle mass. We find that, for $\eta = 0.09$ and $\Lambda = 0.02$, the pair correlation function (PCF) at a density $\rho \sim 1$ and at temperature $T \sim 0.1$ is nearly indistinguishable from that of the classical system. Unless otherwise specified, we use this value of Λ in our simulations (we also present, for comparison, some results obtained with $\Lambda = 0.04$).

A sample of raw simulation data for $\eta = 0.0935$ is reported in Fig. 2. Here, we plot the pressure P as a function of ρ at $T = 0.08$; as evidenced by the two van der Waals loops in $P(\rho)$, upon compression the vapor undergoes two first-order phase transitions. The liquidlike character of the two denser phases, referred to as $L1$ and $L2$, is demonstrated by the PCF (see Fig. 2 inset), which is less structured for the phase of higher density ($L2$).

Figure 3 shows the computed phase diagram of the quantum DG model for three values of η (0.093, 0.0935, and 0.0938) with $\Lambda = 0.02$, and for $\eta = 0.0935$ with $\Lambda = 0.04$. The phase behavior of distinguishable quantum particles (black dots in Fig. 3) mimics that of classical particles. On the other hand, the Bose system displays a much richer phase diagram. Far away from η_c [panel (a)] the only phase transition present is between vapor and liquid, with the liquid becoming superfluid below the Berezinskii-Kosterlitz-Thouless (BKT) line, very much like, e.g., two-dimensional ^{4}He [49,50]. Close to η_c, a second liquid phase appears ($L2$), which coexists with the low-density liquid ($L1$) between a temperature T_t and an η-dependent critical temperature T_c [panels (b) and (c)]. Below T_t, the $L2$ phase instead coexists with the vapor, and a cusp on the saturated $L2$ line at the triple temperature T_t marks this change. The $L2$ phase acquires superfluid properties below the BKT line, which hits the saturated $L2$ line close to T_t (we have to say more on this later). As η_c is approached more and more closely, the $L2$-$L1$ and $L2$-vapor regions become increasingly wider, pushing the

entire saturated $L2$ line toward higher densities. This feature is enhanced in a system with more significant quantum effects, i.e., characterized by a greater value of Λ [panel (d)]. An analysis of the structure and superfluidity of $L2$ droplets in vapor is reported in [38]. Furthermore, we found no trace of cluster solids, in accordance with numerical simulations of Gaussian-core bosons in 2D [51].

A first-order LLPT is unusual for one-component Bose fluids with isotropic interaction, if not even novel. It is an exquisitely quantum phenomenon made possible by particle indistinguishability and favored (at temperatures slightly larger than T_t) by the disparity in structure between a normal liquid of nonoverlapping particles ($L1$, $\rho \approx 1$) and a denser, almost structureless liquid ($L2$). As long as cluster crystals are absent, we expect that a LLPT will be a generic occurrence in a Bose fluid near collapse.

Next, we explore the quantum nature of the $L2$ liquid as a function of temperature, by computing the superfluid fraction along a number of isochores. Typical results are plotted in Fig. 4, reporting f_s data for a few sizes in the case $\eta = 0.0935$, $\Lambda = 0.04$, and $\rho = 4$. The standard way of estimating the superfluid transition temperature T_{BKT} is by using the BKT recursive relations [see, for instance, Ref. [49]). In two different cases (corresponding to the two lower panels in Fig. 3) we find that the BKT line is well approximated by the expression $T_{\mathrm{BKT}} \approx \Lambda\rho$ (reduced units), which is based on the well-known "universal jump" condition [52] and has been shown to afford quantitatively accurate predictions of T_{BKT} in rather different 2D Bose systems, even in the presence of long-ranged interactions [53,54]. This criterion suggests the BKT line will in some cases intersect the saturated $L2$ line above T_t, e.g., for $\eta = 0.0935$ and $\Lambda = 0.04$, where in a range of temperatures above T_t the DG model would then exhibit a first-order liquid-to-superfluid transition. This exciting finding raises the prospect of a coexistence between normal-liquid and superfluid states, which, to our knowledge, has hitherto never been observed in a (real or model) quantum fluid.

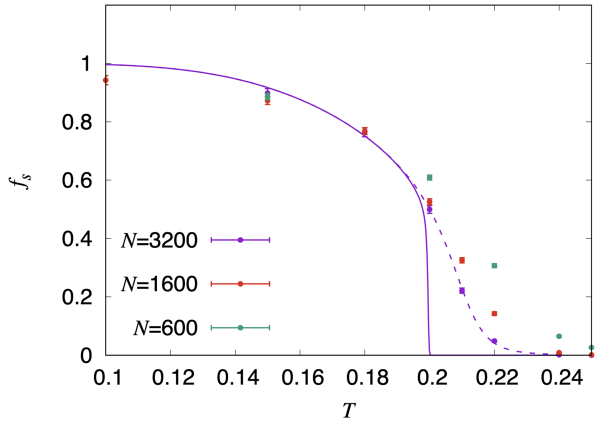

FIG. 4. Superfluid fraction vs temperature for $\eta = 0.0935$, $\Lambda = 0.04$ and $\rho = 4$. Data for various sizes are compared (see legend). The dashed line is a fit through the data for the biggest size. The continuous line is an extrapolation to infinite size based on Kosterlitz-Thouless theory (see, e.g., Ref. [49]).

As for the behavior of the model in the unstable regime, we consider the case $\eta = 0.2$. For the classical model, at $T = 1$ or larger we find the same phenomenology described in Ref. [28], that is, the existence of a characteristic density $\rho_\times(T)$, increasing with T, marking the crossover from a region of full-blown instability on the high-density side, where the collapse of a fluid sample occurs very fast, to a region of apparent stability, where the system remains homogeneous for times longer than the duration of the simulation (see more in [38]). Considering then the quantum DG fluid at $T = 0.1$, collapse of the sample into a compact cluster invariably occurs, even at a density as low as 0.0001. The final cluster looks indistinguishable from a circular droplet in equilibrium, were it not for the scaling of its size and energy with N: while the area of ordinary droplets is an extensive property, the radius of the cluster emerging from the decay of an unstable fluid is almost independent of N; simply, the cluster grows in density when N is increased, while its total energy scales as N^2 [38].

In conclusion, we consider a strongly interacting, two-dimensional Bose fluid in the proximity of collapse. To achieve this, the interparticle potential must be finite at the origin and have an attractive component of adequate strength. To prevent the occurrence of cluster crystals at high density we assume a DG interaction (as representative of a broader class of potentials with the same characteristics [38]). We find that the phase behavior of the nearly unstable system is unusual, in that it undergoes an unprecedented type of LLPT. The denser liquid ($L2$) becomes superfluid when cooled below the BKT line; on the other hand, the low-density liquid ($L1$) is only stable above the BKT line, therefore the BKT transition only occurs for $L2$. As the interaction potential is tuned toward the stability threshold, the $L2$ phase is shifted to higher and higher densities. Finally, the physics of the DG fluid can be observed in a system of ultracold bosons weakly dressed with a Rydberg state; specifically, the atoms should be tailored, in a range of distances well beyond the atomic diameter, with a Q^+-type repulsion [37] and a short-range attraction of generic shape. In this case, stability is recovered, but in an interval of densities below freezing the liquid phase will exhibit essentially the same features present in the DG fluid. We look forward to seeing this scenario realized in future cold-atom platforms.

Acknowledgments—F. C. acknowledges financial support from PNRR MUR Project No. PE0000023-NQSTI. M. B. acknowledges support from the Natural Sciences and Engineering Research Council of Canada. G. P. acknowledges the Center for High Performance Computing (CHPC, South Africa) for providing support within the program MATS088.

[1] H. Tanaka, Liquid-liquid transition and polyamorphism, J. Chem. Phys. **153**, 130901 (2020).

[2] P. H. Poole, F. Sciortino, U. Essmann, and H. E. Stanley, Phase behaviour of metastable water, Nature (London) **360**, 324 (1992).

[3] V. V. Vasisht, S. Saw, and S. Sastry, Liquid-liquid critical point in supercooled silicon, Nat. Phys. **7**, 549 (2011).

[4] C. Pierleoni, M. A. Morales, G. Rillo, M. Holzmann, and D. M. Ceperley, Liquid-liquid phase transition in hydrogen by coupled electron-ion Monte Carlo simulations, Proc. Natl. Acad. Sci. U.S.A. **113**, 4953 (2016).

[5] Y. Katayama, T. Mizutani, W. Utsumi, O. Shimomura, M. Yamakata, and K.-i. Funakoshi, A first-order liquid-liquid phase transition in phosphorus, Nature (London) **403**, 170 (2000).

[6] G. Monaco, S. Falconi, W. A. Crichton, and M. Mezouar, Nature of the first-order phase transition in fluid phosphorus at high temperature and pressure, Phys. Rev. Lett. **90**, 255701 (2003).

[7] L. Henry, M. Mezouar, G. Garbarino, D. Sifré, G. Weck, and F. Datchi, Liquid-liquid transition and critical point in sulfur, Nature (London) **584**, 382 (2020).

[8] H. Tanaka, R. Kurita, and H. Mataki, Liquid-liquid transition in the molecular liquid triphenyl phosphite, Phys. Rev. Lett. **92**, 025701 (2004).

[9] P. C. Hemmer and G. Stell, Fluids with several phase transitions, Phys. Rev. Lett. **24**, 1284 (1970).

[10] E. A. Jagla, Liquid-liquid equilibrium for monodisperse spherical particles, Phys. Rev. E **63**, 061501 (2001).

[11] G. Franzese, G. Malescio, A. Skibinsky, S. V. Buldyrev, and H. E. Stanley, Generic mechanism for generating a liquid-liquid phase transition, Nature (London) **409**, 692 (2001).

[12] V. Molinero, S. Sastry, and C. A. Angell, Tuning of tetrahedrality in a silicon potential yields a series of monatomic (metal-like) glass formers of very high fragility, Phys. Rev. Lett. **97**, 075701 (2006).

[13] F. Smallenburg, L. Filion, and F. Sciortino, Erasing no-man's land by thermodynamically stabilizing the liquid-liquid transition in tetrahedral particles, Nat. Phys. **10**, 653 (2014).

[14] P. G. Debenedetti, F. Sciortino, and G. H. Zerze, Second critical point in two realistic models of water, Science **369**, 289 (2020).

[15] N. Henkel, R. Nath, and T. Pohl, Three-dimensional roton excitations and supersolid formation in Rydberg-excited Bose-Einstein condensates, Phys. Rev. Lett. **104**, 195302 (2010).

[16] J. Zeiher, R. van Bijnen, P. Schauß, S. Hild, J.-y. Choi, T. Pohl, I. Bloch, and C. Gross, Many-body interferometry of a Rydberg-dressed spin lattice, Nat. Phys. **12**, 1095 (2016).

[17] M. Boninsegni, Supersolid phases of cold atom assemblies, J. Low Temp. Phys. **168**, 137 (2012).

[18] F. Cinti, T. Macrì, W. Lechner, G. Pupillo, and T. Pohl, Defect-induced supersolidity with soft-core bosons, Nat. Commun. **5**, 3235 (2014).

[19] M. Ciardi, F. Cinti, G. Pellicane, and S. Prestipino, Supersolid phases of bosonic particles in a bubble trap, Phys. Rev. Lett. **132**, 026001 (2024).

[20] Y. Pomeau and S. Rica, Dynamics of a model of supersolid, Phys. Rev. Lett. **72**, 2426 (1994).

[21] F. Cinti, P. Jain, M. Boninsegni, A. Micheli, P. Zoller, and G. Pupillo, Supersolid droplet crystal in a dipole-blockaded gas, Phys. Rev. Lett. **105**, 135301 (2010).

[22] S. Saccani, S. Moroni, and M. Boninsegni, Phase diagram of soft-core bosons in two dimensions, Phys. Rev. B **83**, 092506 (2011).

[23] S. Prestipino and P. V. Giaquinta, Ground state of weakly repulsive soft-core bosons on a sphere, Phys. Rev. A **99**, 063619 (2019).

[24] M. E. Fisher and D. Ruelle, The stability of many-particle systems, J. Math. Phys. (N.Y.) **7**, 260 (1966).

[25] D. Ruelle, *Statistical Mechanics: Rigorous Results* (W. A. Benjamin, Inc., New York, 1969).

[26] D. M. Heyes and G. Rickayzen, The stability of many-body systems, J. Phys. Condens. Matter **19**, 416101 (2007).

[27] R. Fantoni, A. Malijevský, A. Santos, and A. Giacometti, Phase diagram of the penetrable-square-well model, Europhys. Lett. **93**, 26002 (2011).

[28] G. Malescio and S. Prestipino, Phase behavior near and beyond the thermodynamic stability threshold, Phys. Rev. E **92**, 050301 (2015).

[29] S. Prestipino and G. Malescio, Characterization of the structural collapse undergone by an unstable system of ultrasoft particles, Physica (Amsterdam) **457A**, 492 (2016).

[30] T. Koch, T. Lahaye, J. Metz, B. Fröhlich, A. Griesmaier, and T. Pfau, Stabilization of a purely dipolar quantum gas against collapse, Nat. Phys. **4**, 218 (2008).

[31] T. Lahaye, J. Metz, B. Fröhlich, T. Koch, M. Meister, A. Griesmaier, T. Pfau, H. Saito, Y. Kawaguchi, and M. Ueda, *d*-Wave collapse and explosion of a dipolar Bose-Einstein condensate, Phys. Rev. Lett. **101**, 080401 (2008).

[32] A. Z. Panagiotopoulos, Direct determination of phase coexistence properties of fluids by Monte Carlo simulation in a new ensemble, Mol. Phys. **61**, 813 (1987).

[33] D. Frenkel and B. Smit, *Understanding Molecular Simulation*, 2nd ed. (Academic Press, New York, 2002).

[34] S. Prestipino, C. Speranza, G. Malescio, and P. V. Giaquinta, Twofold reentrant melting in a double-Gaussian fluid, J. Chem. Phys. **140**, 084906 (2014).

[35] C. Speranza, S. Prestipino, G. Malescio, and P. V. Giaquinta, Phase behavior of a fluid with a double Gaussian potential displaying waterlike features, Phys. Rev. E **90**, 012305 (2014).

[36] S. Prestipino, F. Saija, and P. V. Giaquinta, Hexatic phase in the two-dimensional Gaussian-core model, Phys. Rev. Lett. **106**, 235701 (2011).

[37] C. N. Likos, A. Lang, M. Watzlawek, and H. Löwen, Criterion for determining clustering versus reentrant melting behavior for bounded interaction potentials, Phys. Rev. E **63**, 031206 (2001).

[38] See Supplemental Material at http://link.aps.org/supplemental/10.1103/PhysRevLett.133.096001 for an analysis of inhomogeneous states, which includes Refs. [39–41].

[39] J. E. Mayer and W. W. Wood, Interfacial tension effects in finite, periodic, two-dimensional systems, J. Chem. Phys. **42**, 4268 (1965).

[40] K. Binder, B. J. Block, P. Virnau, and A. Tröster, Beyond the van der Waals loop: What can be learned from simulating Lennard-Jones fluids inside the region of phase coexistence, Am. J. Phys. **80**, 1099 (2012).

[41] S. Prestipino, C. Caccamo, D. Costa, G. Malescio, and G. Munaò, Shapes of a liquid droplet in a periodic box, Phys. Rev. E **92**, 022141 (2015).
[42] M. Boninsegni, Nikolay Prokof'ev, and B. Svistunov, Worm algorithm for continuous-space path integral Monte Carlo simulations, Phys. Rev. Lett. **96**, 070601 (2006).
[43] M. Boninsegni, N. V. Prokof'ev, and B. V. Svistunov, Worm algorithm and diagrammatic Monte Carlo: A new approach to continuous-space path integral Monte Carlo simulations, Phys. Rev. E **74**, 036701 (2006).
[44] E. L. Pollock and D. M. Ceperley, Path-integral computation of superfluid densities, Phys. Rev. B **36**, 8343 (1987).
[45] P. Sindzingre, M. L. Klein, and D. M. Ceperley, Path-integral Monte Carlo study of low-temperature ^{4}He clusters, Phys. Rev. Lett. **63**, 1601 (1989).
[46] Y. Kwon, F. Paesani, and K. B. Whaley, Local superfluidity in inhomogeneous quantum fluids, Phys. Rev. B **74**, 174522 (2006).
[47] R. Feynman, *Statistical Mechanics: A Set of Lectures*, Advanced Books Classics (Avalon Publishing, New York, 1998).
[48] Y. Kora, M. Boninsegni, D. T. Son, and S. Zhang, Tuning the quantumness of simple Bose systems: A universal phase diagram, Proc. Natl. Acad. Sci. U.S.A. **117**, 27231 (2020).
[49] D. M. Ceperley and E. L. Pollock, Path-integral simulation of the superfluid transition in two-dimensional ^{4}He, Phys. Rev. B **39**, 2084 (1989).
[50] M. C. Gordillo and D. M. Ceperley, Path-integral calculation of the two-dimensional ^{4}He phase diagram, Phys. Rev. B **58**, 6447 (1998).
[51] P. Kroiss, M. Boninsegni, and L. Pollet, Ground-state phase diagram of Gaussian-core bosons in two dimensions, Phys. Rev. B **93**, 174520 (2016).
[52] D. R. Nelson and J. M. Kosterlitz, Universal jump in the superfluid density of two-dimensional superfluids, Phys. Rev. Lett. **39**, 1201 (1977).
[53] A. Filinov, N. V. Prokof'ev, and M. Bonitz, Berezinskii-Kosterlitz-Thouless transition in two-dimensional dipole systems, Phys. Rev. Lett. **105**, 070401 (2010).
[54] C. Zhang, B. Capogrosso-Sansone, M. Boninsegni, N. V. Prokof'ev, and B. V. Svistunov, Superconducting transition temperature of the Bose one-component plasma, Phys. Rev. Lett. **130**, 236001 (2023).

SUPPLEMENTAL MATERIAL

This document contains further results on the two-dimensional DG model, both classical and quantum, with special reference to inhomogeneous (droplet) states.

Classical model

First, we illustrate the behavior of the classical DG fluid for $\eta = 0.0935$ in the liquid-vapor coexistence region at $T = 0.003$, with the aim to characterize the structure of a liquid droplet at low temperature. After preparing the system at $\rho = 0.1$, we compress it gradually in steps, waiting for the fluid to reach equilibrium at each density. In Fig. 5 (top panels) we show typical configurations for $\rho = 0.25, 0.4$ and 0.45, where the particles are distinguished based on the number of nearest neighbors. Clearly, the system forms a liquid droplet floating in vapor (the vapor density is nearly zero at the temperature considered). Upon increasing ρ, the originally circular droplet grows in area until, due to periodic boundary conditions and the requirement that the free energy (bulk + interface) be minimum [39–41], it changes shape, becoming slab-like. A similar outcome is found at $T = 0.001$ (bottom panels), where the vapor coexists with the triangular solid. Notice the difference in the spatial distribution of coordination defects (disclinations) between the two temperatures: while point defects are diffuse in the liquid droplets, especially far away from the surface, disclinations are less numerous in the solid droplets, where they preferentially form chains of dislocations (grain boundaries).

We note that the density of the droplets in Fig. 5 is slightly below 1. In these conditions, the particle cores are non-overlapping (i.e., the average distance between two neighboring particles is slightly larger than σ), despite being

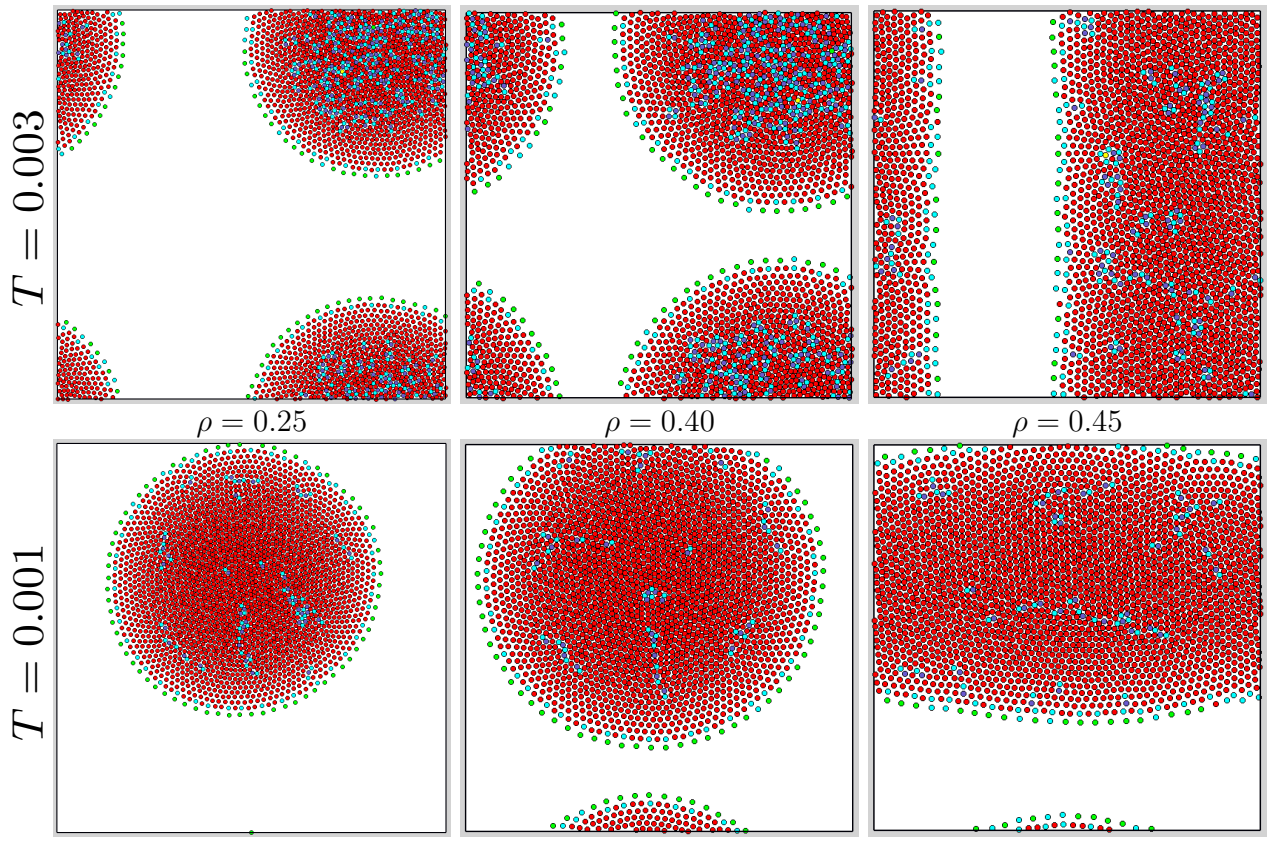

FIG. 5. Two-dimensional classical DG model ($N = 2500$): system snapshots at $T = 0.003$ (top, inside the liquid-vapor region) and $T = 0.001$ (bottom, inside the solid-vapor region), for three densities (from left to right, $\rho = 0.25$, 0.4 and 0.45). Each particle is represented as a circle of diameter σ. Circles are colored according to the particle coordination z, as established via the Voronoi construction: $z \leq 4$ (green); $z = 5$ (cyan); $z = 6$ (red); $z = 7$ (grey); $z \geq 8$ (yellow).

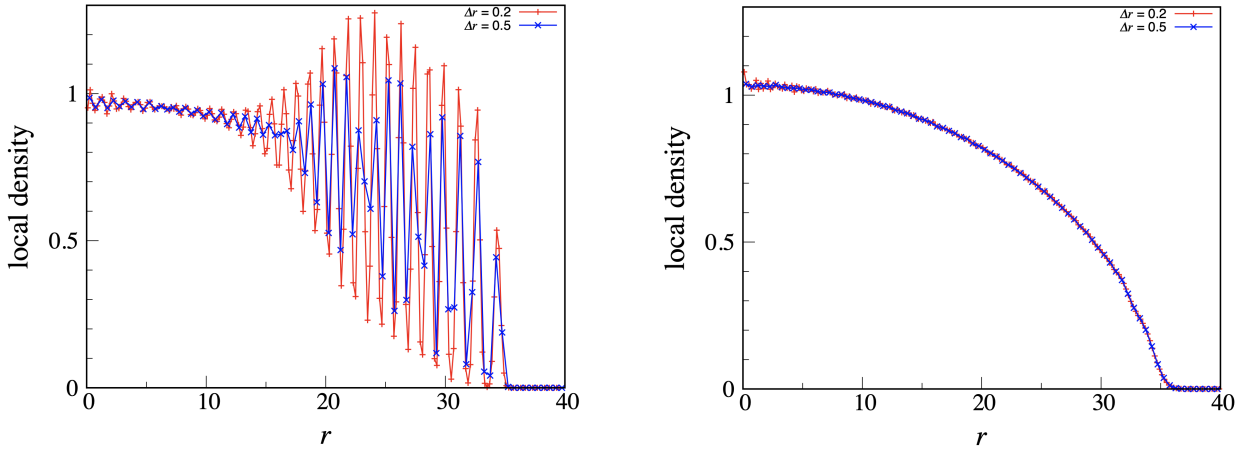

FIG. 6. Two-dimensional classical DG model ($N = 2500$): local density vs (reduced) distance from the droplet center for two liquid-vapor coexistence points. Left: $T = 0.003$ and $\rho = 0.40$. Right: $T = 0.02$ and $\rho = 0.20$. The data are reported using bins of two different widths (in the legend).

penetrable; therefore, the core repulsion is quite effective at these densities. We need substantially higher pressures in the liquid to see the cores overlapping significantly. Eventually, for $\rho \gg 1$ the liquid system becomes a "high-density ideal gas" [37], i.e., a liquid with negligible correlations between the particle positions.

We then look at the profile of the local density, plotted as a function of the distance from the (current) center of mass, in the liquid droplet at $T = 0.003$. By averaging over a large number of equilibrium configurations, the radial profile in Fig. 6a finally emerges. As is also evident in the droplet portrayed in the top-center panel of Fig. 5, the crust of the droplet has an onion-like structure with nearly perfect triangular order, propagating down to approximately half of the droplet radius. On the other hand, in the core of the droplet (where most of the disclinations occur) the local density is smoother, assuming in the center the same value of the density of the saturated liquid at $T = 0.003$ (≈ 0.95, see Fig. 1). In Fig. 6b, the same calculation is repeated for $T = 0.02$. The local density is now very smooth, also near the surface, where the layering effect has almost disappeared.

Next, we investigate the evolution toward collapse in the two-dimensional DG system with $\eta = 0.2$, using the method of molecular dynamics. The sample is initially prepared in a fluid configuration of density $\rho = 1.5$ and temperature $T = 0.2$. If the final state is to be a collapsed configuration of low temperature, the original configuration — of much higher potential energy — is incompatible with a microcanonical dynamics. We have thus decided to put an upper cutoff on the largest displacement that a particle can suffer in one time step, so as to ensure that the system can gradually get rid of the excess potential energy, while keeping the variation in kinetic energy small during the run. An example of system evolution is shown in the enclosed movies, which refer to $N = 4000$. Here, a homogeneous fluid is seen to quickly transform in a few circular clusters of nearly equal radius; at this point, a slower process begins, akin to Ostwald ripening, where the number of clusters is progressively reduced one by one through successive coalescing events, until a unique cluster is finally left. In particular, when two clusters come close to each other, the particles of one cluster are rapidly absorbed by the other cluster; however, the emerging cluster has still the same radius of the two original clusters, hence its density is just the sum of the original densities.

Considering four different sample sizes ($1000, 2000, 4000$, and 8000), we confirm that the gyration radius of the final cluster is 7.91(1), regardless of N, and the total potential energy U scales as N^2 (Fig. 7a). For a cluster of $N = 4000$ particles, we plot in Fig. 7b the local density as a function of the distance from the cluster center. Surprisingly, wide oscillations are superimposed to an overall decreasing profile, becoming sharper near the cluster surface.

We have verified that at $\rho = 0.1$ the system collapse proceeds more slowly, taking a time that is one-two orders of magnitude longer than at $\rho = 1.5$, via the rapid formation of 10-20 clusters which will subsequently coalesce by successive pair-collision events, until only one cluster survives. A similar phenomenology is observed in Monte Carlo simulations.

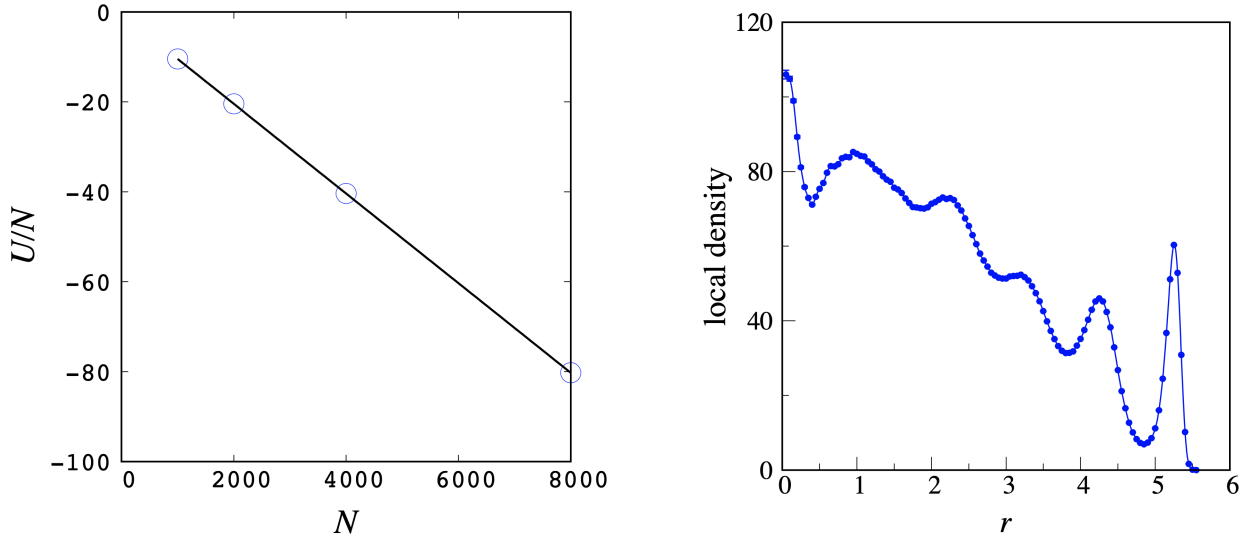

FIG. 7. Classical DG system after collapse at $T = 0.2$ and $\rho = 1.5$ ($\eta = 0.2$): (a) Energy scaling of the total potential energy per particle. (b) Local number density vs distance from the cluster center ($N = 4000$). The statistical uncertainties are smaller than the size of the symbols.

Quantum model

Below the triple-point temperature $T_t \simeq 0.07$ for $\eta = 0.0935$ and $\Lambda = 0.02$, a vapor of nearly zero density coexists with the L2 phase. At very low temperature, say $T = 0.01$, the L2 phase is superfluid in the bulk, with a density of about 3 at coexistence. In these conditions, we have run Quantum Monte Carlo simulations for various N values, starting with a blob of particles and waiting for it to expand until forming a stable droplet. While we expect the same outcome from the simulation of a homogeneous fluid in a very large box ($\rho \ll 1$), our procedure has the distinct advantage of not being necessary to wait for the coalescence of many different condensation nuclei. In Fig. 8a we plot the local density of four stable droplets as a function of the distance from the center. Unexpectedly, the density profile is highly dependent on N, indicating a strong finite-size effect. In particular, the density value in the center of the droplet is much lower than 3, but it increases with N. We have tried to guess the minimum N needed in order that the density becomes 3 in the center, and concluded that this size is likely in the range from 10^4 to 10^5, by far

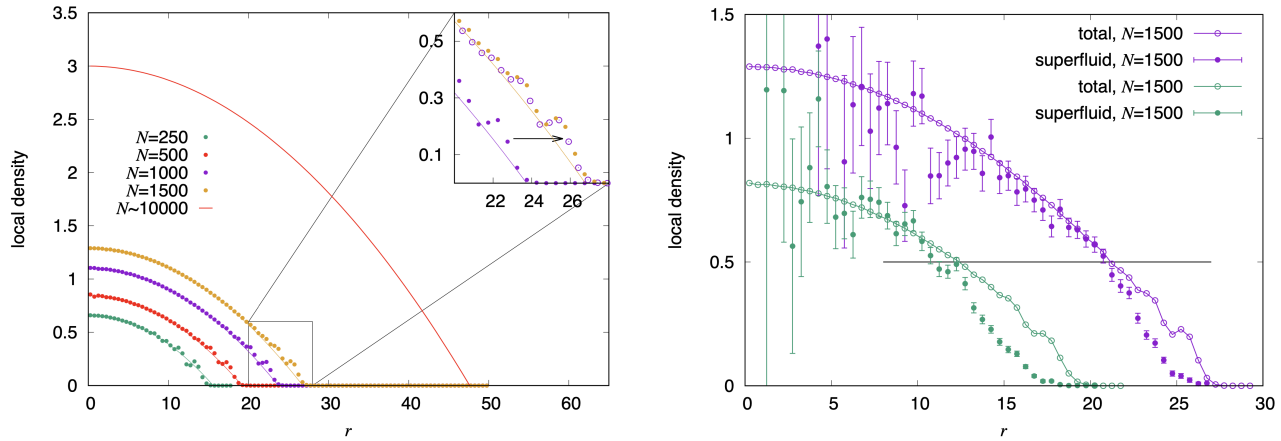

FIG. 8. Two-dimensional quantum DG model at $T = 0.01$ ($\eta = 0.0935$): (a) Radial profile of the local density for various N values (see legend). In the inset, we show a magnification of the surface region, which demonstrates the close similarity between the density modulations for different sizes. (b) Total and superfluid densities as a function of the distance from the center for $N = 500$ and $N = 1500$. The horizontal segment marks the density $\rho = T/\Lambda = 0.5$ (see text).

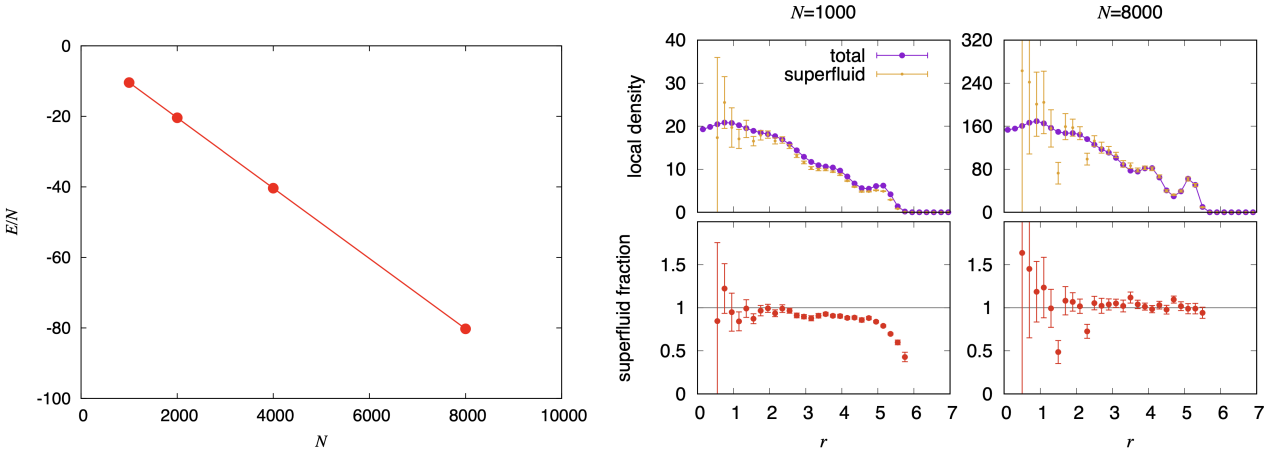

FIG. 9. Quantum DG model at $T = 0.1$ ($\eta = 0.2$). (a) Energy scaling of the total energy per particle. (b) Total and superfluid densities for two collapsed configurations (left: $N = 1000$; right: $N = 8000$).

too much for a direct verification with simulation. Looking at Fig. 8a, we also see a modulation of the density near the droplet surface, occurring in the same terms for all N.

We now turn to consider the nature of the liquid phase in the droplet at $T = 0.01$. We plot in Fig. 8b the total density and the superfluid density as functions of the distance from the droplet center for two distinct sizes, marking with a segment the density level corresponding to the fulfillment of the condition $T = \Lambda\rho$. In spite of the noise affecting the superfluid density data in the droplet core, we clearly recognize that the superfluid fraction is roughly 1 above the segment, while dropping to much lower values below. Hence, we see here reproduced under inhomogeneous conditions the same scenario discussed in the main text: in the region below the locus $T = \Lambda\rho$ on the ρ-T plane (i.e., for densities larger than T/Λ), the liquid acquires superfluid character.

Finally, we take the case of an unstable bosonic fluid at $T = 0.1$ ($\eta = 0.2$). We have verified that, like in the classical-system case, (a) the size of the collapsed configuration (a circular cluster) is independent of N and (b) the total energy per particle scales as N (Fig. 9a). We have also looked at the radial profiles of the total and superfluid densities in the clusters with $N = 1000$ and $N = 8000$ particles (Fig. 9b). Despite the number of particles being quite different, and up to a factor of 8 ($= 8000/1000$) difference, the profiles of both densities are largely overlapping between the clusters. Similar to Fig. 7b, the density profile is modulated, particularly near the surface; with the only visible exception of a thin surface layer for $N = 1000$, where the local density takes small values, the superfluid fraction is practically one at every distance, implying that the collapsed system is entirely superfluid.

On the degree of generality of DG behavior

As we argue below, the same physics of the DG fluid also applies for core repulsions other than Gaussian. When the Fourier transform of the short-range repulsion is positive-definite, the Fourier transform of the total potential function will be positive as well, as long as the attractive part is weak enough, which is the prerequisite for an exact evaluation of the stability threshold based on the two theorems mentioned in the text.

For example, the behavior of the DG model also belongs to a system of bosons interacting through a modified Van der Waals (mVdW) interaction given by $\epsilon\sigma^6/(r^2+\sigma^2)^3$, plus the same attraction as in (1). The mVdW potential is a more realistic shape of softly repulsive core [15] than the Gaussian potential. For any non-negative integer n, the two-dimensional Fourier transform of $\epsilon\sigma^{2(n+1)}/(r^2+\sigma^2)^{n+1}$ is $(2\pi\epsilon\sigma^2/n!)(k\sigma/2)^n K_n(k\sigma)$, where $K_n(x)$ is a modified Bessel function of the second kind (notice that $K_n(x) > 0$ and $(x/2)^n K_n(x) \sim (n-1)!/2$ for $x \to 0$ and $n > 0$). The stability threshold of the potential combining the mVdW repulsion ($n = 2$) with the attractive component of (1) is exactly half of the DG threshold. It is worth observing that, at variance with the mVdW repulsion, the two-dimensional Fourier transform of a repulsive core modeled as $\epsilon\sigma^6/(r^6+\sigma^6)$ [15] has no definite sign.